



OPEN ACCESS

EDITED BY

Laurent Coppola,
UMR7093 Laboratoire d'océanographie de
Villefranche (LOV), France

REVIEWED BY

Leticia Cotrim Da Cunha,
Rio de Janeiro State University, Brazil
Nicolas Metzl,
Centre National de la Recherche Scientifique
(CNRS), France

*CORRESPONDENCE

Ricardo Arruda
✉ cadoarruda@gmail.com

RECEIVED 29 July 2024

ACCEPTED 08 October 2024

PUBLISHED 25 October 2024

CITATION

Arruda R, Atamanchuk D, Boteler C
and Wallace DWR (2024) Seasonality
of $p\text{CO}_2$ and air-sea CO_2 fluxes
in the Central Labrador Sea.
Front. Mar. Sci. 11:1472697.
doi: 10.3389/fmars.2024.1472697

COPYRIGHT

© 2024 Arruda, Atamanchuk, Boteler and
Wallace. This is an open-access article
distributed under the terms of the [Creative
Commons Attribution License \(CC BY\)](#). The
use, distribution or reproduction in other
forums is permitted, provided the original
author(s) and the copyright owner(s) are
credited and that the original publication in
this journal is cited, in accordance with
accepted academic practice. No use,
distribution or reproduction is permitted
which does not comply with these terms.

Seasonality of $p\text{CO}_2$ and air-sea CO_2 fluxes in the Central Labrador Sea

Ricardo Arruda^{1*}, Dariia Atamanchuk¹, Claire Boteler²
and Douglas W. R. Wallace¹

¹Department of Oceanography, Dalhousie University, Halifax, NS, Canada, ²Department of Mathematics and Statistics, Dalhousie University, Halifax, NS, Canada

The Labrador Sea in the subpolar North Atlantic is known for its large air-to-sea CO_2 fluxes, which can be around 40% higher than in other regions of intense ocean uptake like the Eastern Pacific and within the Northwest Atlantic. This region is also a hot-spot for storage of anthropogenic CO_2 . Deep water is formed here, so that dissolved gas uptake by the surface ocean directly connects to deeper waters, helping to determine how much atmospheric CO_2 may be sequestered (or released) by the deep ocean. Currently, the Central Labrador Sea acts as a year-round sink of atmospheric CO_2 , with intensification of uptake driven by biological production in spring and lasting through summer and fall. Observational estimates of air-sea CO_2 fluxes in the region rely upon very limited, scattered data with a distinct lack of wintertime observations. Here, we compile surface ocean observations of $p\text{CO}_2$ from moorings and underway measurements, including previously unreported data, between 2000 and 2020, to create a baseline seasonal climatology for the Central Labrador Sea. This is used as a reference to compare against other observational-based and statistical estimates of regional surface $p\text{CO}_2$ and air-sea fluxes from a collection of global products. The comparison reveals systematic differences in the representation of the seasonal cycle of $p\text{CO}_2$ and uncertainties in the magnitude of air-sea CO_2 fluxes. The analysis reveals the paramount importance of long-term, seasonally-resolved data coverage in this region in order to accurately quantify the size of the present ocean sink for atmospheric CO_2 and its sensitivity to climate perturbations.

KEYWORDS

$p\text{CO}_2$, air-sea CO_2 fluxes, observation, seasonality, Labrador Sea

1 Introduction and objectives

The ocean is the main reservoir that regulates atmospheric CO_2 concentrations at short to long time scales, (10 - 1000 years), due to the exchange of CO_2 at the air-sea interface over the large area of the global ocean, and the enormous capacity for carbon storage in the water column (DeVries, 2022). Globally, it has been estimated that the oceans have

absorbed between 30% to 50% of the CO₂ emitted due to human activity since the onset of the industrial revolution (Sabine et al., 2004; Gruber et al., 2019), thus damping the effects of rising atmospheric CO₂ concentrations on climate (Friedlingstein et al., 2022). However, ocean CO₂ uptake estimates and seasonal variability of fluxes and carbon-state variables (*p*CO₂, DIC and Total Alkalinity) differ from global biogeochemical models and observation-based data products, particularly at high latitudes (Hauck et al., 2023; Rodgers et al., 2023; Pérez et al., 2024).

The Labrador Sea is an important area of the ocean with one of the world's highest rates of influx of atmospheric CO₂, along with other high-latitude regions such as areas of the Arctic Ocean (e.g. Baffin Bay, Davis Strait, Chukchi Sea) (Bates and Mathis, 2009; Ahmed et al., 2019; Duke et al., 2023a) and Greenland Sea (Nakaoka et al., 2006; Olsen et al., 2008). Moreover, other regions exhibiting moderate to intense influx of atmospheric CO₂ are present in highly dynamic coastal areas on continental shelves within middle to high latitudes (Laruelle et al., 2014; Landschützer et al., 2020).

Within the Central Labrador Sea, deep-reaching and highly variable mixing of the water column occurs annually through deep convection (Marshall and Schott, 1999; Curry and McCartney, 2001), with the mixed layer depth (MLD) extending as deep as 2000 meters during winter (Kieke and Yashayaev, 2015; Yashayaev and Loder, 2017). This convection contributes to the formation of a major water mass, the North Atlantic Deep Water (NADW), which enters into the Atlantic Meridional Overturning Circulation (Fu et al., 2020) and exports them, eventually, to other oceanic basins (Körtzinger et al., 2004; Zantopp et al., 2017; Koelling et al., 2022). The deep mixed layer in the Central Labrador Sea connects the atmosphere to intermediate and deep waters through a “trap-door” that opens briefly during the fall/winter deep convection events and is closed during the stratified spring/summer seasons (Atamanchuk et al., 2020). Overall, this region presents a year-round sink of atmospheric CO₂, with intensification during summer and fall, and limited net exchange in winter (Körtzinger et al., 2008a; Atamanchuk et al., 2020).

The Central Labrador Sea has been shown to have a very high column inventory of anthropogenic carbon (Sabine et al., 2004; Khatiwala et al., 2013; DeVries, 2014; Gruber et al., 2019) and a storage rate that outpaces the global average and is variable in time (Terenzi et al., 2007), with an average rate of increase of around 1.8 mol m⁻² year⁻¹ for the last three decades (Raimondi et al., 2021; Steinfeldt et al., 2024). Therefore, this region may also expect rapid ocean acidification impacts on marine life in the deep ocean (Azetsu-Scott et al., 2010). On the other hand, the large fluxes combined with the sensitivity of deep mixing to high-latitude oceanic changes (shallowing of mixed layer depths/weakening of overturning circulation) may put at risk the ocean's future ability to mitigate climate change by storing anthropogenic CO₂.

Historically, when compared to adjacent more observed regions, the coverage of partial pressure of CO₂ (*p*CO₂) observations within the Central Labrador Sea has been insufficient to constrain the air-sea CO₂ fluxes, given the region's high variability (e.g. Friedrich and Oschlies, 2009a). The AR07W GO-SHIP repeat hydrography line has been a key source of data with discrete observations of carbon-system parameters, including *p*CO₂,

together with physical, chemical and biological variables, which have been collected annually since 1992 (Hall et al., 2013; Raimondi et al., 2019). However, there is a strong seasonal bias in the sampling along AR07W, with most of the data collected in spring/summer (mostly in May and June), and no data collected during winter months. There is also limited spatial resolution inherent in the ship-based discrete sampling along a single section.

Complementing the AR07W data, a few sporadic transits by research vessels equipped with underway *p*CO₂ measurement systems have taken place between 2000 and 2020. However, these measurements were also taken almost exclusively in summer and fall. Some are included in the SOCAT database from 2021 (SOCATv2021, Bakker et al., 2016).

The seasonal variability of *p*CO₂ in this region has, however, also been observed from four mooring deployments: in 2000/2001 (DeGrandpre et al., 2006), in 2004 (Martz et al., 2009), in 2004/2005 (Körtzinger et al., 2008a) and most recently with the SeaCycler deployment in 2016/2017 (Atamanchuk et al., 2020). The mooring data provide much needed, high-resolution temporal coverage encompassing multiple seasons but are not included in the SOCAT database (except the mooring from 2004 - Martz et al., 2009). Previously, it had been suggested, based on model analysis, that the addition of even a single long-term mooring could decrease the error of estimates of air-sea fluxes by about 20% for the region (Friedrich and Oschlies, 2009a), but the hypothesis has not been tested against actual measurements.

The combination of ocean surface *p*CO₂ observations using underway measurements from Ships of Opportunity (SOOP), research vessels, autonomous surface vehicles (e.g. Waveglider, Saildrone, Sailbuoy) and from moorings will be key for further investigation of the spatio-temporal *p*CO₂ variability and reducing uncertainties of the estimates of air-sea CO₂ fluxes (Hauck et al., 2023). Mooring and buoy deployments are important for improving the temporal coverage (winter gap in observations), and underway measurements are crucial for improving spatial coverage. The combination of these different types of observations is particularly important in high-latitude regions such as the Central Labrador Sea, which is a highly dynamic region with poor data coverage.

A variety of statistical and mapping techniques have been developed for interpolation and extrapolation of *p*CO₂ observations and air-sea CO₂ fluxes estimates, including into regions that have limited or no data. These include statistical interpolation (Takahashi et al., 2002, 2009), multiple linear regression (MLR) with more extensively-measured variables (Schuster et al., 2013; Iida et al., 2015) and neural network approaches (Chen et al., 2019). The neural network reconstructions have been applied at regional (Xu et al., 2019; Wrobel-Niedzwiecka et al., 2022; Duke et al., 2024), basin (Friedrich and Oschlies, 2009a, b; Telszewski et al., 2009; Landschützer et al., 2013), and global scales (Zeng et al., 2014; Landschützer et al., 2016; Laruelle et al., 2017; Denvil-Sommer et al., 2019; Roobaert et al., 2024).

Even though a wide range of gap-filling techniques have been applied, these remain observation-based approaches and therefore, ultimately, the accuracy and uncertainties of all these techniques rely on data coverage (Rödenbeck et al., 2015; Gloege et al., 2021).

Results from some of these approaches will be used here as a comparison with our new observation-based climatology. Although there are shortcomings when comparing studies with different resolutions and different time-spans, such comparisons can be useful to identify systematic errors and specific locations in global and basin-scale estimates that could benefit from additional targeted observations.

These comparison studies can also help guide future development of long-term observation strategies (such as initiatives for new mooring deployments or Ship of Opportunity (SOOP) lines). Also, for data-poor regions such as the Central Labrador Sea, a relatively small addition of observations has potential to improve or validate the estimates from gap-filling methods considerably, both regionally and even possibly for basin-scale estimate of fluxes (Friedrich and Oschlies, 2009a).

Here we have compiled $p\text{CO}_2$ observations, including previously unavailable data sets, from the Central Labrador Sea. Given that data availability in any particular year was low, we combined and adjusted all available $p\text{CO}_2$ data collected over two decades to the single year 2020, which was the most recent year with available data (see Methods). The combined observations are used to create a climatology of $p\text{CO}_2$ and air-sea CO_2 fluxes, which is then used as a reference for regional comparisons and validations against several global products that used gap-filling techniques and extrapolation. Taking into account the discrepancies arising from these comparisons and the data coverage problems in this important region for CO_2 uptake and storage, we make recommendations for future monitoring and research.

2 Methods

We define the seasonality of surface $p\text{CO}_2$ in the Central Labrador Sea, making use of the unusually rich mooring-based data set from this region in combination with underway observations available from the SOCATv2021 database (Bakker et al., 2016). We also highlight and include some observations not available in SOCATv2021 (named here as “non-SOCAT”). These include four crossings of the Central Labrador Sea between the years 2000–2020 by the research vessels CCGS Amundsen (General Oceanics $p\text{CO}_2$ system) and CCGS Hudson (Pro-Oceanus Systems’ - membrane-based). From the SOCATv2021 database only two crossings are available over this 21 year time-period, and the newer versions of SOCAT (v2022 and v2023) did not add any new observations in the Central Labrador Sea for the time span of this study. This reiterates the general lack of data availability for this region. Of the four mooring deployments, data from only one is currently included in SOCATv2021 (from Martz et al., 2009).

The data coverage around the Central Labrador Sea is also illustrated here (Figure 1), showing the addition of the “non-SOCAT” observations (between 2017 and 2020; CCGS Amundsen and CCGS Hudson cruises and observations within the Atlantic continental shelves). We have quality-controlled all of these additional observations and some are submitted to the SOCAT database. By adding these preliminary “non-SOCAT” data we can

anticipate how the data coverage will improve in the next versions of SOCAT, and more importantly, highlighting where and when observations are needed within the Labrador Sea.

2.1 Study area

Our study focuses on a limited region of the Central Labrador Sea, spanning from 55.5°N to 57.5°N and from 51.5°W to 53.5°W (orange box, Figure 1). The specific area selected was based on mapping of past deep convection events (Marshall and Schott, 1999), which has led to deployments of several moorings in this location, and is believed to be representative of a significant area of the deeper mixing within the Central Labrador Sea. However, the deep convection activity in the Central Labrador is also known to be dynamic, and there is inter-annual variability of the area of deep water formation (Rühs et al., 2021). The red box in Figure 1 shows, for comparison, the resolution of early global-based $p\text{CO}_2$ products produced by Takahashi et al., 2002 and Takahashi et al., 2009 (4°x5° grid). In contrast, a smaller grid cell (2°x2°) was chosen for analysis in this study to exclude data-points collected over the continental shelves and slopes that surround the Central Labrador Sea.

The “non-SOCAT” underway measurements presented and utilized here (see Figure 1) are from the Atlantic Zone Off-Shore Monitoring Program (AZOMP) and Atlantic Zone Monitoring Program (AZMP) of Canada’s Department of Fisheries and Oceans (DFO), with both programs taking place on-board CCGS Hudson, between 2016 and 2019 (CCGS Hudson data submitted to SOCAT versions 2023 and 2024). Further, underway measurements collected from the CCGS Amundsen are also included in this study, with data from 2017 to 2020 (pending submission to SOCAT). Finally, observations over the Atlantic continental shelves (data: Cyr et al., 2022; Gibb et al., 2023) are also included in Figure 1 (Labrador Shelf area) to show possible opportunities for future expansion of the Canadian $p\text{CO}_2$ observation network. All of these “non-SOCAT” data were quality controlled and are either submitted or pending submission to newer versions of the SOCAT database (Supplementary Table 4 in Supplementary Materials). In the meantime they can be requested from the authors listed in the data availability section of this manuscript.

Within the grid cell chosen in this study (approximately 50,000 km², orange box, Figure 1), the “non-SOCAT” underway data includes three crossings (13 days of observations), from the years 2015, 2016 and 2018. In comparison, the SOCATv2021 dataset includes only two crossings of the area (four days of observations), from 2008 and 2016.

It is important to point out the importance of the mooring datasets presented here (details in Table 1) that made this study possible due to the temporal/seasonal coverage that they provide in comparison to ship-based studies. When ship-based underway-observations are so sporadic and limited, observations from mooring deployments become essential. The discussion in the remainder of this paper focuses on the data collected within the 2°x2° orange box in the Central Labrador Sea (Figure 1).

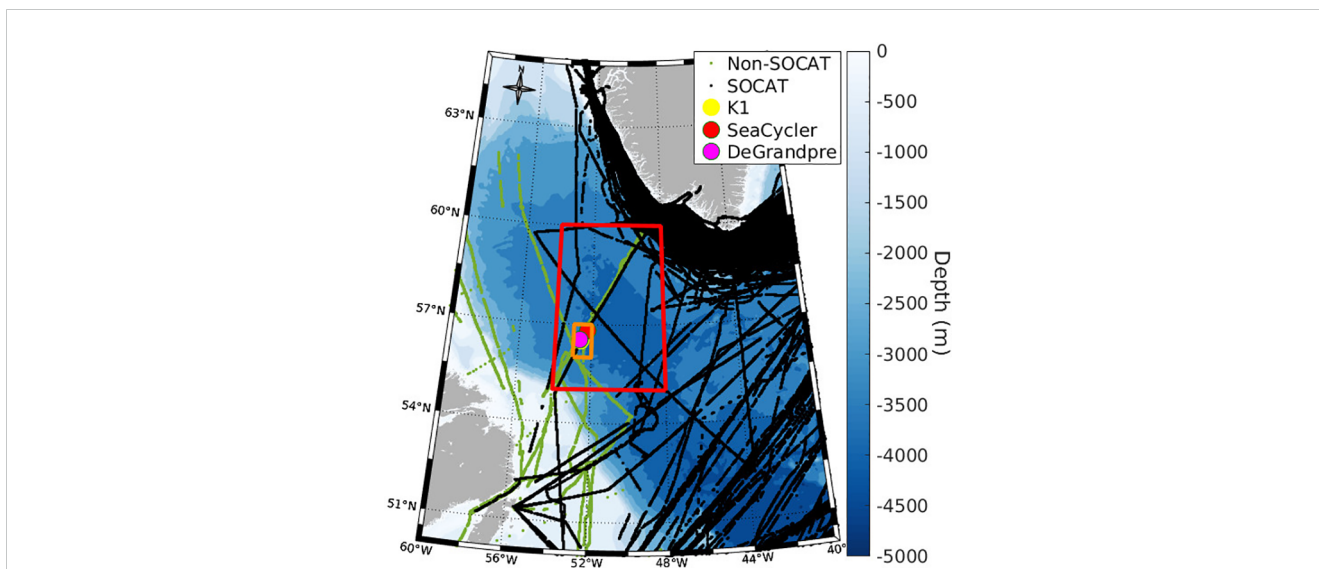


FIGURE 1
 Location of area of interest in the Central Labrador Sea (orange box), showing the mooring locations (circles) and the underway data from SOCATv2021 (black) and the “non-SOCAT” (green) available for the region between 2000 and 2020. The red box shows the 4°x5° grid cell of the Takahashi climatologies.

2.2 pCO₂ data sources and flux calculations

The global pCO₂ products compared here are the climatologies of Takahashi et al. (2002); Takahashi et al. (2009) and Fay et al. (2023) (discussed in Fay et al., 2024); these climatologies are referred to here as T2002, T2009 and T2023, respectively. The T2023 climatology is provided as ΔfCO₂, we therefore recalculated fCO₂ by adding the atmospheric fCO₂ (for reference year 2010 as in Fay et al., 2024), and converted to pCO₂ using surface temperature (Weiss, 1974) for the reference year 2010 (Multi Observation Global Ocean ARMOR3D L4 – Copernicus - Guinehut et al., 2012).

We also compare six other observation-based products from the harmonization of pCO₂ products provided by Gregor and Fay (2021) and discussed in Fay et al. (2021), which includes multiple linear regression models (MLR), machine learning ensemble (ML6), mixed layer scheme (MLS) and three neural network-based models (references and details of each product are given in Table 2). All these products used SOCAT observations for reconstruction of pCO₂ on a model grid.

We calculated a regional pCO₂ climatology directly from pCO₂ observations and compared it with the climatologies calculated from the pCO₂ global products. We also used the pCO₂ observations and pCO₂ from each of the global products to

TABLE 1 Details of mooring deployments in the Central Labrador Sea.

Mooring	Start of deployment	End of deployment	Depth	Seasonal coverage (number of unique months)	Average pCO ₂ ± 1 STD (uatm)	summer -min (uatm)	winter-max (uatm)	Precision (uatm)	Type of Sensor
DeGrandpre et al., 2006	June, 2000	June, 2001	Surface layer	1 (Mooring sank, only using data before it sank)	325.6 ± 36.6	256.9	No winter data	± 5	SAMI-CO ₂
Körtzinger et al., 2008a (K1)	September, 2004	July, 2005	Surface layer	11	386.4 ± 24.8	317.6	420.7	± 5 to 10	SAMI-CO ₂
Martz et al., 2009	June, 2004	August, 2004	Near surface	3 (mooring drifted – not included here. Data included in SOCATv2021, but outside the area of interest)	325.6 ± 16.1	293.1	No winter data	± 5	SAMI-CO ₂
Atamanchuk et al., 2020 (SeaCycler)	May, 2016	May, 2017	Near surface	9 (Profiling mooring, only using surface data in this study)	331.3 ± 30.8	255.1	412.4	± 10	Pro-Oceanus CO ₂ -Pro CV

TABLE 2 Details of the products used to compare the seasonality of $p\text{CO}_2$ in the Central Labrador Sea.

Product	Gap filling method	Resolution	Mean $p\text{CO}_2 \pm 1 \text{ STD}$	summer – min $p\text{CO}_2$	winter – max $p\text{CO}_2$	Amplitude	Average BIAS	MAE	RMSE	Database used
Takahashi et al., 2002 (T2002)	Interpolation	4/5 degrees	363.41 \pm 33.33	301.36	405.82	104.46	- 9.42	12.44	17.31	LDEO (1956-2000)
Takahashi et al., 2009 (T2009)	Advection-based Interpolation	4/5 degrees	352.66 \pm 13.73	325.03	367.13	42.10	-20.17	27.51	33.42	LDEO (1970 - 2006)
Fay et al., 2023 (T2023)	Interpolation	1/1 degrees	384.12 \pm 34.74	308.45	426.67	118.22	11.29	29.98	33.79	SOCAT v2022
Landschützer et al., 2017 (MPI)	NN	1/1 degrees	355.23 \pm 37.47	263.31	413.57	150.26	-17.60	21.02	29.53	SOCAT v5
Gregor et al., 2019 (CSIR)	ML6	1/1 degrees	358.54 \pm 30.58	271.24	398.16	126.92	-14.29	16.47	22.77	SOCAT v5
Zeng et al., 2014 (NIES)	NN	1/1 degrees	358.38 \pm 46.60	282.22	433.75	151.53	-14.45	22.82	30.67	SOCAT v2
Chau et al., 2022 (CMEMS)	NN	1/1 degrees	357.28 \pm 36.89	261.76	404.45	142.69	-15.54	18.22	25.06	SOCAT v2020
Rödenbeck et al., 2013 (JENA)	MLS	1/1 degrees	358.72 \pm 28.19	267.59	416.15	148.56	-14.10	18.71	22.13	SOCAT v1.5
Iida et al., 2021 (JMA)	MLR	1/1 degrees	359.46 \pm 37.11	278.47	428.67	150.20	-13.37	21.24	27.28	SOCAT v2019
Observation-based (this study)	-	-	386.36 \pm 34.65	255.12	453.09	197.97	-	-	-	SOCAT v2021 + additional observations

Showing mean, minimum and maximum values (in μatm). Also showing metrics for each comparison: average BIAS, Mean Absolute Error (MAE) and Root Mean Squared Error (RMSE). Gap filling methods: Neural Networks (NN), machine learning ensemble (ML6) and mixed layer scheme (MLS). Values in bold for the observation-based estimates of this study.

calculate air-sea CO₂ fluxes, and consequently the climatologies of the fluxes.

The air-sea CO₂ fluxes ($FCO_2^{(air-sea)}$) were calculated using the following equation (Equation 1):

$$FCO_2^{(air-sea)} = kCO_2 K_0 (pCO_2^{(air)} - pCO_2^{(sea)}), \quad (1)$$

where kCO_2 is the transfer velocity according to Wanninkhof (1992), K_0 is the solubility constant following Weiss (1974), with $pCO_2^{(air)}$ and $pCO_2^{(sea)}$ as the atmospheric and ocean surface pCO_2 . From here on we will use $\Delta pCO_2 = pCO_2^{(air)} - pCO_2^{(sea)}$. The air-sea flux is dependent on the transfer velocity (kCO_2), which is strongly dependent on wind speed. Since we are dealing with a data-poor region, we fixed the choice of wind product and wind parameterization in order to focus on the effect of pCO_2 data-coverage. Specifically, we used wind speed estimates from the reanalysis product ERA5 (Hersbach et al., 2020), which has been widely used in global products, including those compared here, due to its high spatio-temporal resolution for the flux calculation (see also Atamanchuk et al., 2020).

We calculated the monthly uncertainty of air-sea CO₂ fluxes (∂FCO_2) by propagating the monthly errors of wind (∂U) and ΔpCO_2 ($\partial \Delta pCO_2$), which we believe to be the largest sources of uncertainties for this climatological approach, using the following equation (Equation 2):

$$\partial FCO_2 = FCO_2 ((\partial U/U)^2 + (\partial \Delta pCO_2 / \Delta pCO_2)^2)^{1/2} \quad (2)$$

2.3 Monthly climatology

The monthly climatology, i.e. the seasonality of sea-surface pCO_2 , was calculated as a monthly average and monthly standard deviation to create our climatological reference for the Central Labrador Sea using pCO_2 observations from 2000 to 2020. The climatology was calculated with the pCO_2 and fluxes data compiled for this study and for each of the global products of monthly time series. We then analyze how well the global products compare with the directly observed seasonal variability of pCO_2 and air-sea CO₂ fluxes in the Central Labrador Sea.

To compile pCO_2 observations collected over 21 years for a climatological monthly averaging approach, it is necessary to correct for the increase in atmospheric (and surface ocean) pCO_2 over time. For that, we used the Icelandic atmospheric time series between 1992 and 2020 (Dlugokencky et al., 2021), as well as observations from Sable Island between 1993 and 2019 (Worthy, 2023). For the Iceland station, an increase of 2.16 $\mu\text{atm}/\text{year}$ was found, and for the Sable Island station there was an increase of 2.08 $\mu\text{atm}/\text{year}$. Both time series showed a similar rate of increase, with the slopes of the two linear least squares regression being statistically indistinguishable ($p\text{-value} > 0.05$). This rate of atmospheric increase used here is consistent with the 2.2 $\mu\text{atm}/\text{year}$ rate reported in Raimondi et al., 2021, for the period 1996–2016 in the same region. Therefore, for simplicity, we used 2.1 $\mu\text{atm}/\text{year}$ for adjusting surface water pCO_2 to the common reference year of 2020.

3 Results and discussion

3.1 Seasonality of observed pCO_2

Figure 1 shows that there are large data gaps throughout most of the Labrador Sea domain, especially in the Central, Northern, and Labrador Shelf regions. We decided to show all observations in and around the study area (even though they are not all used in our analysis) to emphasize the major observational gap that exists in this region, despite the region's potential significance for exchange of gases and carbon between the atmosphere and the deep ocean. Even with the addition of the “non-SOCAT” data presented here, we are still far from having anything close to representative observational coverage for the Northwestern Atlantic Ocean, including the Labrador Sea (Central and Northern) and Canadian shelves (see Duke et al., 2023b).

The pCO_2 data from the Central Labrador Sea moorings (Figure 1; Table 1) show a strong seasonal cycle (Figure 2), with relatively high, near-equilibrium pCO_2 in winter (JFM) weakening the uptake of atmospheric CO₂, and low pCO_2 values in spring (AMJ) and summer (JAS), increasing the difference with the atmospheric pCO_2 and thus driving a strong CO₂ sink. The timing of the decline in pCO_2 in mid-spring (referred to here as the “spring-decline”) varies from year to year, and a second less pronounced drop in pCO_2 may occur in the fall (OND) as well. This overall seasonality is driven partly by biological activity, including a strong decrease of pCO_2 coinciding with the start of the spring bloom, and partly by abiotic controls (i.e. changes in temperature and vertical mixing) as pCO_2 increases steadily after summer until the end of winter. As the wintertime cooling sets in, increased solubility would drive CO₂ fluxes into the ocean, however, the deepening of the mixed layer carrying a high pCO_2 signal from respiration are mixed into the surface layer, thus driving CO₂ fluxes out of the ocean (outgassing) (Körtzinger et al., 2008a; Martz et al., 2009). This will lead to a maximum winter-time pCO_2 as observed in other high latitude regions (Iida et al., 2015).

The variability of our pCO_2 climatology increases after including the underway observations with the mooring data in the analysis, however the overall seasonality remains consistent and well represented (Figure 2), with the expected high pCO_2 in winter ($409 \pm 7 \mu\text{atm}$), followed by a steep decline through spring until mid-summer, when it reaches the minimum in July (down to 250 μatm). After averaging all available data, both from moorings and underway systems, we can confirm that over the entire seasonal cycle the region acts as a year-around sink for atmospheric pCO_2 (i.e. $pCO_2^{(sea)} < pCO_2^{(air)}$). There are only a few days when ocean surface pCO_2 may exceed atmospheric pCO_2 , and this may happen right before the “spring-decline”, when observations show increased variability (during May and June).

As seen in Figure 2, even after the inclusion of the underway observations, the majority of the observations discussed here come from the three mooring deployments, showing their major importance for this otherwise under-sampled region. Using the monthly average of the pCO_2 observations shown in Figure 2, we produced an estimate for the seasonal climatology for the Central Labrador Sea, which is used as the reference “observation-based” climatology.

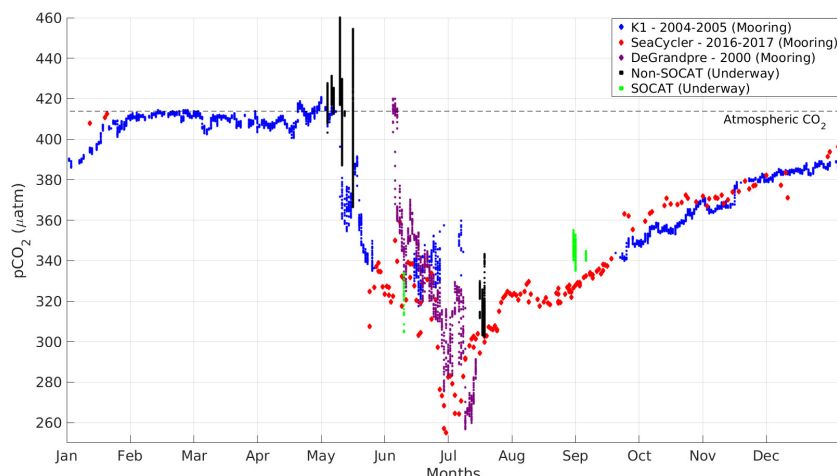


FIGURE 2

Daily averages of all $p\text{CO}_2$ observations from the 3 moorings, and from underway measurements (both SOCAT and “Non-SOCAT”). All values are corrected to the year 2020 (adjusted for an atmospheric increase of 2.1 $\mu\text{atm}/\text{year}$). Located within the orange box in Figure 1. Horizontal dotted line showing average atmospheric $p\text{CO}_2$ for 2020 (Copernicus Atmosphere Monitoring Service – CAMS).

3.2 Comparison of $p\text{CO}_2$ observations against global products

When comparing $p\text{CO}_2$ seasonal climatologies from the different global products (Figures 3, 4), they also characterize the Central Labrador Sea as a region of atmospheric CO_2 uptake (sink). Most products follow the overall pattern seen in the observations (Figure 2). However, the timing and amplitude of the seasonal cycle of $p\text{CO}_2$ is not consistent between the products and the observational data. For example, most products indicate an earlier “spring-decline” of $p\text{CO}_2$ compared to the observation-based estimate (March/April vs May, Figure 2). There is also a shift of timing of the summer minimum (earlier summer minimum, except

in Takahashi et al. (2009), that shows a minimum in August). Most of the products underestimate $p\text{CO}_2$ in winter, spring and summer when compared to the observation-based estimate (black line), with a bias (product - observations) over time ranging from -80 to +40 μatm (Figure 4). To a lesser degree, there is also an overestimation of $p\text{CO}_2$ by most products in late-summer and fall. The products MPI, JENA, NIES and JMA showed the highest seasonal amplitudes (winter maximum – summer minimum) of around 150 μatm , the observation-based estimate however showed an even higher amplitude of almost 200 μatm .

We note an especially strong difference between the two early Takahashi climatologies (Takahashi et al., 2002, 2009), with the seasonality from Takahashi et al. (2009) being the least consistent

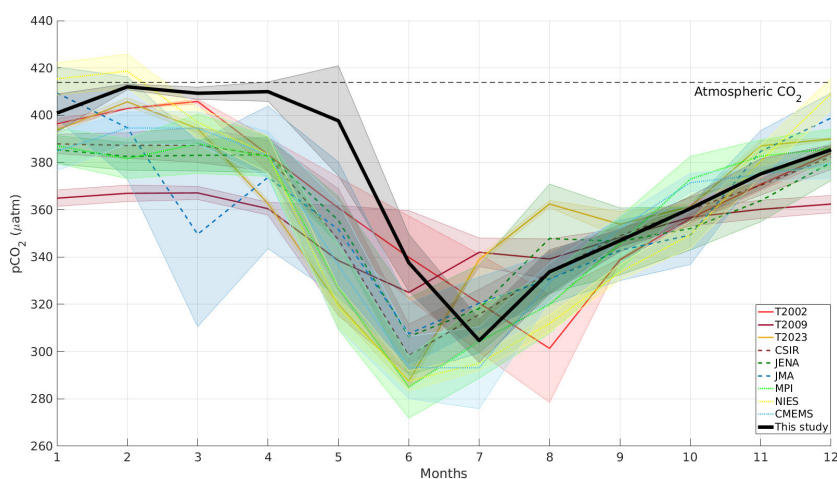


FIGURE 3

Comparison of climatologies of Takahashi 2002 (T2002), Takahashi 2009 (T2009), Fay et al., 2023 (T2023) and 6 observational-based global products discussed in Fay et al. (2021), with original references presented in Table 2. Comparison for the Central Labrador Sea – located within the orange box in Figure 1 (except for T2002 and T2009 – within red box). Solid lines are the monthly climatologies, shaded areas showing ± 1 standard deviation. Black line shows the observation-based product (this study). All data have been corrected to the year 2020. The horizontal dotted line shows the average atmospheric $p\text{CO}_2$ for 2020 (Copernicus Atmosphere Monitoring Service – CAMS).

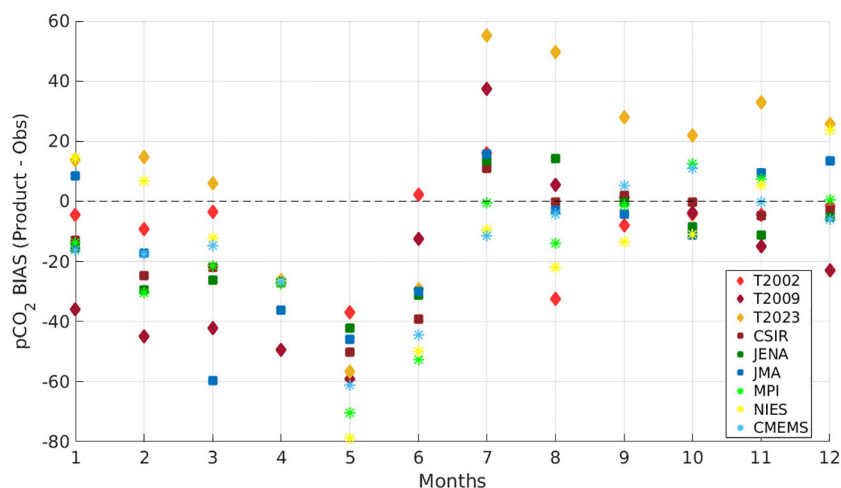


FIGURE 4

Bias over time of $p\text{CO}_2$ (Product – Observation) for the 9 global products and the observation-based climatology compared in this study (in μatm). Diamonds are the climatologies from Takahashi, squares are products that used multiple linear regressions, and * are neural network-based products.

with observations and with the other global products. These differences may be due to the different extrapolation techniques combined with the fast increase in observations of $p\text{CO}_2$, with the new observations being mostly on the border of the $4^\circ \times 5^\circ$ grid (see Figure 1, red box) around the Greenland shelf and slope by the Nuka Arctica underway system (Olsen et al., 2008), therefore potentially skewing the expected seasonality of the Central Labrador Sea for this climatology.

We keep these earlier Takahashi climatologies in the discussion since they have been used as benchmarks for comparisons in earlier studies (e.g. Lüger et al., 2004; Körtzinger et al., 2008b; Landschützer et al., 2014; Lauderdale et al., 2016). The new Takahashi climatology (T2023 - Fay et al., 2023) shows a better seasonal cycle (based on SOCATv2022 with more observations available), agreeing with the other products, although showing an early increase in $p\text{CO}_2$ in the summer, and an overestimation of $p\text{CO}_2$ from summer through fall. Other more recent gap-filling methods discussed in the study may, however, be more appropriate for this regional scale analysis due to their finer resolution, although they also have their strengths and weaknesses based on statistical metrics.

Of the $p\text{CO}_2$ products with a $1^\circ \times 1^\circ$ degree resolution, the CSIR product (Gregor et al., 2019) has the lowest mean absolute error (MAE) and root mean square error (RMSE) related to the observation-based climatology of this study (MAE=16.5 μatm ; RMSE=30.7 μatm). This is influenced by its summer-fall values being almost equal to our observation-based product (MAE=3.56 μatm). The CSIR winter-spring values are underestimated compared to the observations, however their bias is on the low-end compared to the other products. The annual average bias was slightly more negative for CSIR (-14.3 μatm) than JMA (-13.4 μatm) (Iida et al., 2021), however further examination of the monthly bias (Figure 4) shows multiple months with positive bias in the fall that will cancel out some of the negative bias in the winter. The higher spread of bias values for the JMA product is reflected in its higher MAE and RMSE (MAE=21.2 μatm ; RMSE=27.3 μatm). Recent

products with finer resolution ($0.25^\circ \times 0.25^\circ$, e.g. Chau et al., 2024; Gregor et al., 2024) could lead to improvements in the results for this region.

Although the data products discussed here are all intended as global-scale products, these should be tested to assess their skill in different basins or even at regional levels, such as in this study. Rödenbeck et al. (2015), for example, recommended checks on the consistency between such products and the use of multiple products in such comparisons.

3.3 Air-sea CO_2 flux comparison

Figure 5 shows the seasonal variability of the calculated air-sea CO_2 fluxes and the comparison of these observation-based estimates with the same global products discussed above. Similar to $p\text{CO}_2$, the majority of estimates of air-sea CO_2 fluxes from the global products indicate a pattern of overestimation from winter to spring and underestimation from summer to fall when compared to the observation-based estimate in this study. The monthly average bias (product - observations) for each global product is shown in Figure 6, ranging from -0.42 to +0.5 $\text{molC m}^{-2}\text{month}^{-1}$, with most products showing stronger fluxes than the observations in the first half of the year (winter: -0.42 to +0.38 $\text{molC m}^{-2}\text{month}^{-1}$; spring: -0.35 to +0.16 $\text{molC m}^{-2}\text{month}^{-1}$), and weaker fluxes in the second half of the year (summer: +0.12 to +0.28 $\text{molC m}^{-2}\text{month}^{-1}$; fall: -0.09 to +0.52 $\text{molC m}^{-2}\text{month}^{-1}$).

Bias values are negative (stronger fluxes than observation-based estimate) for winter-spring and positive (weaker fluxes than observation-based estimate) for summer-fall. The seasonal positive and negative biases tend to cancel out, thus leading many products to have an annual average bias that is low. Hence the mean absolute error (MAE) and RMSE metrics (see Table 3) are more appropriate for discussion here. Of the $1^\circ \times 1^\circ$ degree products, CMEMS, JENA and JMA show the lowest MAE and RMSE. The

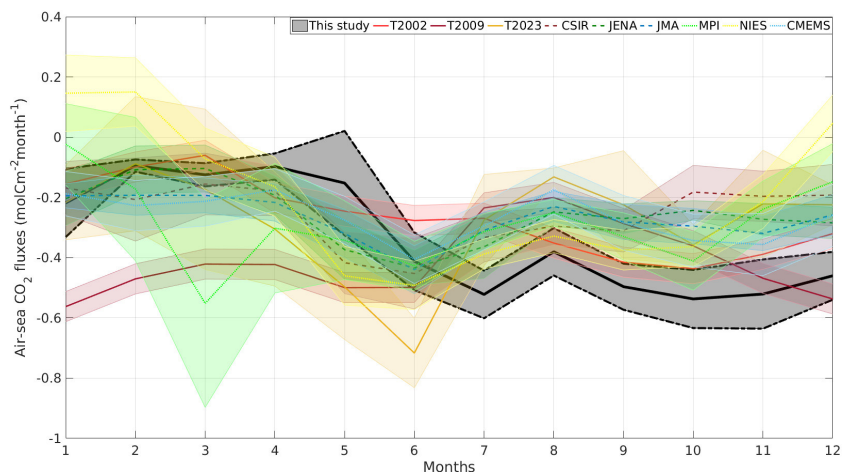


FIGURE 5
Comparison of climatologies of air-sea CO₂ fluxes. Solid lines are the monthly climatologies, shaded areas showing ± 1 standard deviation. Dashed black-lines are showing upper and lower limits of fluxes calculated by uncertainty propagation of pCO₂ and wind.

climatology from Takahashi et al., 2002 also shows good metrics when compared to the observations, which does not hold for the newer version of Takahashi et al., 2009 (T2009), as shown in Figures 6, 7. Notably, T2009 stands out from the other products in showing a strong overestimation of fluxes during winter. The climatology from Fay et al., 2023 (T2023) shows a slight improvement in the metrics when compared to T2009 (T2023 includes additional observations from SOCATv2022). Overall, the JMA product has the lowest bias, however the MAE and RSME metrics in both pCO₂ and flux suggest the CMEMS, JENA and JMA as the best options when compared to the reference observation-based climatology.

When averaged seasonally, summer and fall are the seasons with the highest fluxes based on observations, and are also the seasons with larger inconsistencies between the global products and

observation-based estimate (Figure 7; Table 3). In the fall, only the T2009 product corresponds closely to the observations (with overlapping error-bars) and in summer, only T2002 and NIES. The NIES product is the only product that classifies the Central Labrador Sea as a source of CO₂ to the atmosphere during winter and shows small positive values (close to equilibrium or a weak source) within the seasonal variability during the fall. The MPI product overall classifies the winter as a sink, but its large uncertainty does not preclude that some winters may have out-gassing periods. T2023 and NIES are the products with higher amplitudes of 0.62 and 0.64 molC m⁻²month⁻¹, respectively. Annually, all products show consistent representation of an ocean sink, with the observation-based estimate being -4.0 ± 2.2 molC m⁻²year⁻¹, and most products showing a slight underestimation of the flux when compared to our observation-based estimate (Figure 8).

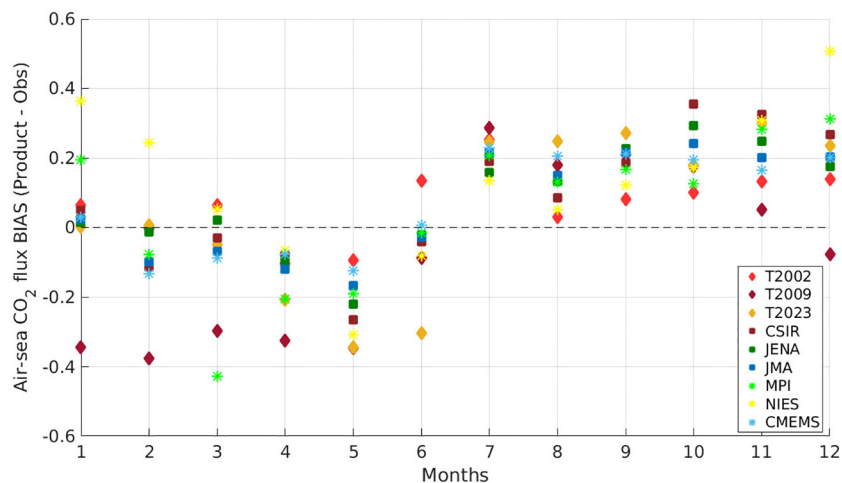


FIGURE 6
Bias over time of air-sea CO₂ fluxes (Product – Observation) for the 9 global products and the observation-based climatology compared in this study (in molC m⁻²month⁻¹). Diamonds are the climatologies from Takahashi, squares are products that used multiple linear regressions, and * are neural network-based.

TABLE 3 Comparison of air-sea CO₂ fluxes in the Central Labrador Sea.

Product	Mean flux ± 1 STD (molC m ⁻² month ⁻¹)	winter –min (Low flux)	summer –max (High flux)	Amplitude	Average BIAS	MAE	RMSE
Takahashi et al., 2002 (T2002)	-0.27 ± 0.12	-0.06	-0.44	0.38	0.07	0.10	0.12
Takahashi et al., 2009 (T2009)	-0.41 ± 0.12	-0.20	-0.56	0.36	-0.08	0.23	0.25
Fay et al., 2023 (T2023)	-0.28 ± 0.17	-0.09	-0.71	0.62	0.05	0.20	0.23
Landschützer et al., 2017 (MPI)	-0.29 ± 0.14	-0.02	-0.55	0.53	0.04	0.19	0.22
Gregor et al., 2019 (CSIR)	-0.26 ± 0.10	-0.15	-0.45	0.30	0.07	0.16	0.22
Zeng et al., 2014 (NIES)	-0.21 ± 0.23	+0.15	-0.49	0.64	0.12	0.20	0.24
Chau et al., 2022 (CMEMS)	-0.26 ± 0.07	-0.17	-0.40	0.23	-0.06	0.13	0.15
Rödenbeck et al., 2013 (JENA)	-0.26 ± 0.10	-0.10	-0.43	0.33	0.08	0.13	0.16
Iida et al., 2021 (JMA)	-0.27 ± 0.07	-0.19	-0.44	0.25	0.06	0.14	0.16
Observation-based (this study)	-0.33 ± 0.18	-0.09	-0.54	0.45	-	-	-

Showing mean, minimum and maximum values. Also showing metrics for each comparison: Amplitude, average BIAS, Mean Absolute Error (MAE) and Root Mean Squared Error (RMSE). Gas exchange parameterization of Wanninkhof (1992) was used for all products. Wind product ERA5 was used for calculation of fluxes. Values in bold for the observation-based estimates of this study.

3.4 Uncertainties of CO₂ fluxes in high latitudes

High latitude regions such as the Labrador Sea are amongst the poorest in terms of pCO₂ data coverage, even while their significance for global air-sea fluxes and net carbon storage is high. Therefore, high latitude regions usually fall within the regions with highest uncertainty and errors in both regional and global gap-filling estimates (Gloege et al., 2021). For example, there remains controversy whether the Southern Ocean acts as a strong or weak sink (Sutton et al., 2021). However, the seasonality at the

regional scales and the strength of the inter-annual variability is poorly characterized, due to large winter-gaps in observations increasing the uncertainty in the Southern Ocean (Mackay et al., 2022; Wu and Qi, 2022). Similarly, in the North Atlantic Ocean, the Labrador Sea is one of the regions with the fewest observations, also leading to high uncertainties.

Here we identify some key sources of uncertainties for the air-sea flux estimates. Firstly, the choice of wind products and wind parametrization for the bulk-formula calculation of CO₂ fluxes are among the most important sources of errors. Different parameterization choices for the gas transfer coefficient can alter

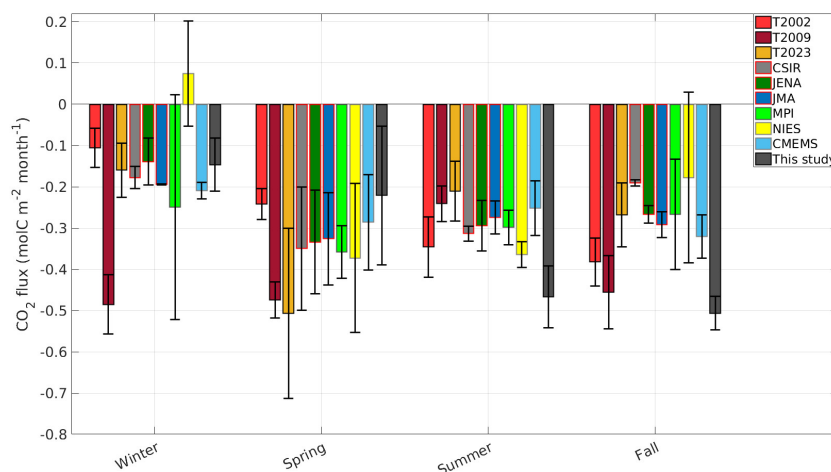


FIGURE 7 Seasonal average of air-sea CO₂ fluxes (error bars showing ± 1 standard deviation) for the 9 global products and the observation-based estimate from this study.

the intensity of the CO₂ fluxes estimates in the region by an average of $\pm 20\%$ or approximately $0.08 \text{ molC m}^{-2}\text{month}^{-1}$ (Atamanchuk et al., 2020). In this study, the parameterization of Wanninkhof (1992) was used for our observation-based reference climatology and for the global products compared in this study.

When using different wind products (e.g. NCEP and CCMP products) with the same parameterization, the observation-based estimates can vary by as much as $-0.17 \text{ molC m}^{-2}\text{month}^{-1}$, notably during the period of strong summer uptake. This can lead to an almost 50% decrease of the intensity of the summertime carbon sink in the Central Labrador Sea, by switching from ERA5 to NCEP. Differences between CCMP and ERA5 are less pronounced, with a maximum difference around $-0.05 \text{ molC m}^{-2}\text{month}^{-1}$ during the summer. Overall, differences between fluxes calculated using these three wind products are largest in summer and fall, and less pronounced in winter and spring, being consistent with the flux formulation and $\Delta p\text{CO}_2$, that is, when air-sea $p\text{CO}_2$ gradient are larger, differences of using different wind products are also more pronounced. In this study, ERA5 was used to calculate CO₂ fluxes, for the estimate presented in this study and for the global products.

The uncertainties of wind products and wind parametrization have been discussed previously (e.g. Moore et al., 2008; Koelling et al., 2017; Woolf et al., 2019; Atamanchuk et al., 2020), and clearly represent a major problem for global estimates of air-sea CO₂ fluxes. Another source of uncertainty is the measurement of the surface temperature, which in most cases occurs at the depth of a ship's intake of water, which is located typically well below the air-sea interface (e.g. at 5–10 m). This implies a need for an adjustment of the temperature (and $p\text{CO}_2$) to reflect actual surface conditions (Watson et al., 2020). Finally, the cool and salty skin-temperature effect offers potential for major bias, with these two factors together having the potential to increase the global oceanic uptake by as much as factor of two (Watson et al., 2020). Other important sources of uncertainties include: (1) uncertainty related to the $p\text{CO}_2$ measurements (Bender et al., 2002; Wanninkhof et al., 2019; Dong

et al., 2024); (2) gap-filling model uncertainties (e.g. data-coverage uncertainty; Duke et al., 2023a); and (3) uncertainty from the wind measurements that feed global wind-products (Roobaert et al., 2018; Chiodi et al., 2019; Wright et al., 2021; Fang and An, 2022).

Figure 9 shows the seasonal relationship of air-sea CO₂ fluxes, $p\text{CO}_2$ (or $\Delta p\text{CO}_2$), surface temperature and wind. The fluxes are more intense and more variable starting in spring, through summer and fall. The contribution of each variable towards predicting the variability of CO₂ fluxes was explored using multiple linear least squares regression. We found $\Delta p\text{CO}_2$ alone was able to describe 62% of the calculated flux variability ($R^2 = 0.62$ and $p\text{-value} = 0.0023$). Based on a regression of CO₂ fluxes with both $\Delta p\text{CO}_2$ and wind, given the amplitude of variability, these two variables were able to describe 84% of the flux variability ($R^2 = 0.84$ and $p\text{-value} = 0.0002$), thus, the variable wind (U) improves the regression together with $\Delta p\text{CO}_2$. However, we found that wind alone cannot explain the variability of fluxes (large $p\text{-value}$). Temperature alone also cannot explain the variability of fluxes in the Central Labrador Sea (large $p\text{-value}$), due to the opposite expected effect of the temperature changes in $\Delta p\text{CO}_2$ and thus in the fluxes as well. Therefore, measurements of surface ocean $p\text{CO}_2$ remains the most important variable for constraining and improving the estimates of air-sea CO₂ fluxes in this region (consistent with this, Dong et al., 2024 found larger standard deviations in reconstructions due to a recent decline in SOCAT observations), followed by resolving/improving the wind (U) data products and parametrization. It is important to point out that these relationships are particular to our region of interest and also dependent on the type of gas exchange parameterization (in this case, using Wanninkhof (1992)).

4 Conclusions and recommendations

This study compiled all available $p\text{CO}_2$ observations from various platforms and different measuring systems, to define the

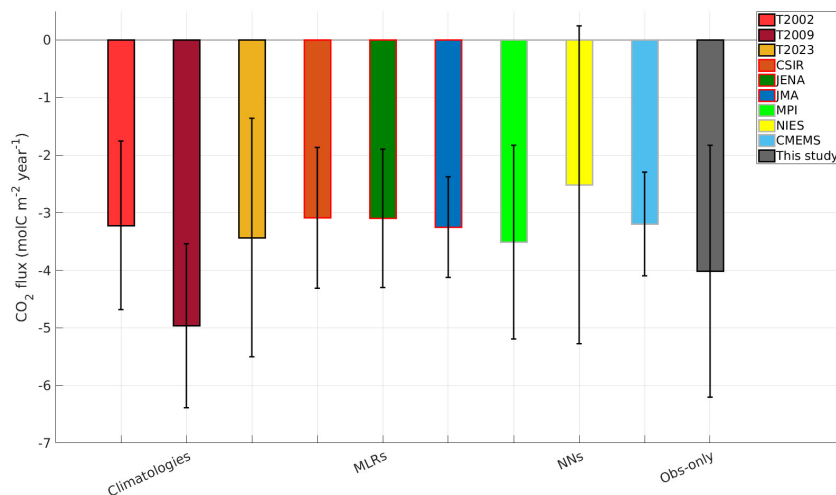


FIGURE 8

Annual average of air-sea CO₂ fluxes (error bars showing ± 1 standard deviation) for the 9 global products and the observation-based estimate from this study.

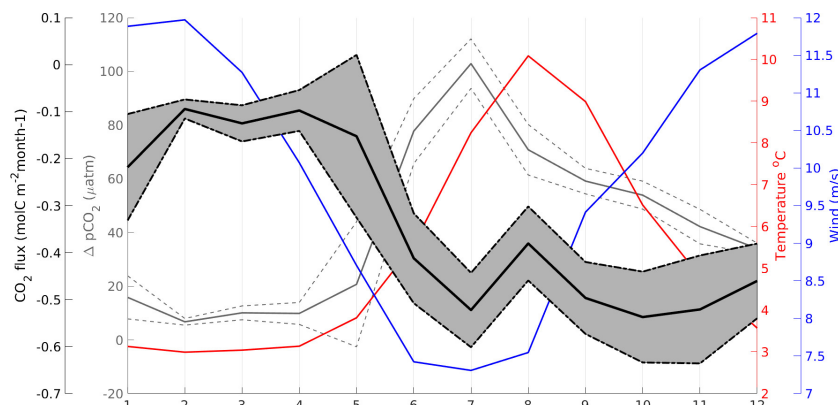


FIGURE 9

Seasonality of observed $\Delta p\text{CO}_2$ and air-sea CO_2 fluxes (observation-based estimate from this study), together with monthly averaged SST and wind. Dotted lines and shaded areas showing ± 1 standard deviation.

seasonal cycle of $p\text{CO}_2$ and air-sea CO_2 fluxes in the Central Labrador Sea. The compilation of observational data creates an observation-based climatology product (referenced to the year 2020), that can be used as a reference for assessing future variability and changes. Furthermore, this reference climatology can be used to skill-test biogeochemical models or gap-filling techniques for their applicability to the Central Labrador Sea.

Since the Central Labrador Sea has very limited data coverage, and a strong seasonal cycle for $p\text{CO}_2$ and air-sea CO_2 fluxes, the data collected from near-surface moorings equipped with $p\text{CO}_2$ sensors, has been key in defining the seasonal cycle.

The comparisons with global $p\text{CO}_2$ data products reveal similarities and some large discrepancies between the products with our observation-based seasonal climatology, both in magnitude (differences ranging up to +40 to -80 μatm) and in the seasonal cycle, especially with respect to the timing of the spring-decline and the spring/summer $p\text{CO}_2$ minimum. This is the period when $p\text{CO}_2$ shows the highest variability and the CO_2 fluxes are most intense.

The $p\text{CO}_2$ amplitude is well captured by most products in late summer and fall, whereas there is strong underestimation of $p\text{CO}_2$ in the winter by most products when compared to observations (lower values than expected), except for the T2023 and NIES climatologies that show overestimation of $p\text{CO}_2$ in winter. The spring/summer minimum also showed an underestimation of $p\text{CO}_2$ when compared to our observation-based climatology. Overall, all products underestimate the seasonal amplitude of $p\text{CO}_2$ variations when comparing to the observation-based estimate presented here (see Table 2).

Air-sea CO_2 flux estimates diverge significantly, even when estimated using a common wind-product (ERA5). On the one hand, the annual averaged fluxes are all consistent with the observation-based estimate (between -0.09 and -0.54 $\text{molC m}^{-2}\text{month}^{-1}$), however they can deviate strongly over the year due to the region's strong seasonality. When averaging the fluxes seasonally, we see a clear problem in winter, with high divergence between the products and the estimates from this study. During

summer and fall, most products underestimated the CO_2 sink and, to a lesser degree, most products showed an overestimation of the CO_2 sink in spring.

The sources of uncertainties when estimating seasonal air-sea fluxes are: observational uncertainty on $p\text{CO}_2$ measurements; wind related uncertainty (different wind products and parameterizations); uncertainty in the gridding/binning of observations; and uncertainty from the statistical or gap-filling method used (i.e. due to poor coverage in space and time).

Our study suggests that it is important to obtain a minimum amount of data (with both seasonal and spatial coverage) in such regions for constraining and validating estimates from gap-filling methods. Data gaps may not only result in the underestimation of variability, but could also lead to the emergence of errors due to sampling biases (Rödenbeck et al., 2015). The observation-based climatology presented here is a step towards increasing the data-coverage in the Central Labrador Sea deep-water formation region. The differences between our observation-based climatological reference and the global products presented here are mainly due to an overall lack of $p\text{CO}_2$ observations in the Central Labrador Sea. Improved target-data ($p\text{CO}_2$) coverage will have positive impacts for variable selection (predictors) in statistical and observation-based methods like neural networks.

Notably, inter-annual variability is not addressed in this study, as the sparse temporal coverage of observations in the Central Labrador Sea makes such an analysis almost impossible, so that we would have to rely on gap-filling methods to do so. Inter-annual variability has been found to only be constrained in the more densely observed regions of the ocean (Rödenbeck et al., 2015) which are, however, not necessarily the regions where such variability is largest. Ultimately, improvement of the accuracy of reconstructions of the ocean carbon sink using gap-filling methods, will require expansion of the scope of both underway and mooring-based observations programs to encompass areas (and seasons) where data is scarce (Denvil-Sommer et al., 2019; Gloege et al., 2021).

This study also shows that $p\text{CO}_2$ data coverage can be expanded slightly in the near-future if the "non-SOCAT" data, such as those

presented here, are made available. However, we recommend addition of new SOOP lines in the Labrador Sea and its continental shelves, including installation of dedicated underway systems in Canadian Research and Coast Guard vessels or commercial vessels that transit the region, as well as deployment of autonomous surface vehicles capable of collecting data on fine time and space-scales. These possibilities for increasing data-coverage in the future, although not necessarily in winter.

We also emphasize the importance of providing data to global databases such as SOCAT, but we note that some of these data in data-poor regions may be derived from new/alternative $p\text{CO}_2$ sensors and unconventional platforms (e.g. moorings) which may be subject to over-critical examination and hence may be, inadvertently, discouraged. Databases and their QA/QC requirements may be biased towards conventional existing measuring systems in their flagging system, but such systems may not necessarily be suited for data collection in remote regions (see also Arruda et al., 2020). Critical examination of the currently accepted standards for $p\text{CO}_2$ data collection and reporting (and their impact), will be required in order to maximize the utility and availability of observations, which will in turn improve the skill of gap-filling techniques. Furthermore, making water column observations of other carbon-state variables such as DIC and total alkalinity available through submission to other databases (e.g. GLODAP) is also important, especially in a region with deep water formation such as the Central Labrador Sea.

We highlight the specific value of long-term mooring deployments equipped with $p\text{CO}_2$ sensors and recommend ongoing efforts to increase deployments of such platforms for improving the winter-gap in data coverage. Also, further investigation/comparison studies of sensor-based $p\text{CO}_2$ observation will be important for increasing data coverage, and we therefore recommend acceptance and expanded discussions of these types of observations by databases such as SOCAT. Finally, we recommend rapid delivery of new observations to SOCAT, regardless of the quality-flag. The additional observations can prove to be extremely helpful in improving or validating the skill of some of the gap-filling techniques compared here.

The broad $p\text{CO}_2$ community involved in both measuring but also analyzing and estimating CO_2 fluxes should work together to place emphasis on data collection in regions with high fluxes, high $p\text{CO}_2$ variability and high flux variability. These highly dynamic regions are usually the same regions where we lack consistent observations (e.g. Arctic, Southern Ocean, South Atlantic tropical and subtropical, and upwelling systems – Canary/Humboldt). Additional observations in these locations may lead to overall improvements in air-sea CO_2 fluxes estimates, possibly reducing the uncertainties in the order of 10-20% (Hauck et al., 2023; Behncke et al., 2024). On another front, we recommend urgent validation of wind-speed products in regions with high CO_2 fluxes, which could reduce the uncertainties from the gas-exchange calculation, and also possibly reduce the differences encountered when estimating air-sea CO_2 fluxes with different wind products.

For the Central Labrador Sea, a unique region that connects the atmosphere with the deep ocean with intense CO_2 fluxes, creating a

reference for seasonality is key for future comparisons within a new ocean state. Overall, the type of compilation provided here can also be useful for pinpointing other regions that would benefit the most from additional $p\text{CO}_2$ observations in the Northwestern Atlantic Ocean.

Data availability statement

The raw data supporting the conclusions of this article will be made available by the authors, without undue reservation.

Author contributions

RA: Conceptualization, Data curation, Formal analysis, Investigation, Methodology, Validation, Visualization, Writing – original draft, Writing – review & editing. DA: Conceptualization, Investigation, Methodology, Resources, Supervision, Writing – review & editing. CB: Formal analysis, Investigation, Methodology, Writing – review & editing. DW: Conceptualization, Funding acquisition, Investigation, Methodology, Project administration, Resources, Supervision, Writing – original draft, Writing – review & editing.

Funding

The author(s) declare financial support was received for the research, authorship, and/or publication of this article. This research was supported by the Ocean Frontier Institute (OFI), through an award from the Canada First Research Excellence Fund, Canada Excellence Research Chair in Ocean Science and Technology (CERC.Ocean) Program and the Natural Sciences and Engineering Research Council of Canada (NSERC) through the Advancing Climate Change Science in Canada program (grant no. ACCPJ 536173-18).

Acknowledgments

We acknowledge the Bedford Institute of Oceanography (BIO-DFO) team led by Kumiko Azetsu-Scott, Darlene Childs and Stephen Punshon for running and operating the $p\text{CO}_2$ underway systems in the AZMP and AZOMP cruises. We acknowledge the support of Arne Körtzinger, Mike DeGrandpre, Brent Else, Frederic Cyr and Todd Martz for providing $p\text{CO}_2$ data. The Surface Ocean CO_2 Atlas (SOCAT) is an international effort, endorsed by the International Ocean Carbon Coordination Project (IOCCP), the Surface Ocean Lower Atmosphere Study (SOLAS) and the Integrated Marine Biosphere Research (IMBeR) program, to deliver a uniformly quality-controlled surface ocean CO_2 database. The many researchers and funding agencies responsible for the collection of data and quality control are thanked for their contributions to SOCAT.

Conflict of interest

The authors declare that the research was conducted in the absence of any commercial or financial relationships that could be construed as a potential conflict of interest.

Publisher's note

All claims expressed in this article are solely those of the authors and do not necessarily represent those of their affiliated organizations, or those of the publisher, the editors and the

reviewers. Any product that may be evaluated in this article, or claim that may be made by its manufacturer, is not guaranteed or endorsed by the publisher.

Supplementary material

The Supplementary Material for this article can be found online at: <https://www.frontiersin.org/articles/10.3389/fmars.2024.1472697/full#supplementary-material>

SUPPLEMENTARY TABLE 4

Details of the non-SOCAT datasets used in this study.

References

- Ahmed, M., Else, B. G. T., Burgers, T. M., and Papakyriakou, T. (2019). Variability of surface water $p\text{CO}_2$ in the Canadian Arctic Archipelago from 2010 to 2016. *J. Geophysical Research: Oceans* 124, 1876–1896. doi: 10.1029/2018jc014639
- Arruda, R., Atamanchuk, D., Cronin, M., Steinhoff, T., and Wallace, D. W. (2020). At-sea intercomparison of three underway $p\text{CO}_2$ systems. *Limnology Oceanography: Methods* 18, 63–76. doi: 10.1002/lom3.10346
- Atamanchuk, D., Koelling, J., Send, U., and Wallace, D. W. R. (2020). Rapid transfer of oxygen to the deep ocean mediated by bubbles. *Nat. Geosci.* 13, 232–237. doi: 10.1038/s41561-020-0532-2
- Azetsu-Scott, K., Clarke, A., Falkner, K., Hamilton, J., Jones, E. P., Lee, C., et al. (2010). Calcium carbonate saturation states in the waters of the Canadian Arctic Archipelago and the Labrador Sea. *J. Geophysical Research: Oceans* 115, p. C11021. doi: 10.1029/2009jc005917
- Bakker, D. C., Pfeil, B., Landa, C. S., Metzl, N., O'Brien, K. M., Olsen, A., et al. (2016). A multi-decade record of high-quality $f\text{CO}_2$ data in version 3 of the Surface Ocean CO_2 Atlas (SOCAT). *Earth System Sci. Data* 8, 383–413. doi: 10.5194/essd-8-383-2016
- Bates, N. R., and Mathis, J. T. (2009). The Arctic Ocean marine carbon cycle: evaluation of air-sea CO_2 exchanges, ocean acidification impacts and potential feedbacks. *Biogeosciences* 6, 2433–2459. doi: 10.5194/bg-6-2433-2009
- Behncke, J., Landschützer, P., and Tanhua, T. (2024). A detectable change in the air-sea CO_2 flux estimate from sailboat measurements. *Sci. Rep.* 14, 3345. doi: 10.1038/s41598-024-53159-0
- Bender, M., Doney, S., Feely, R. A., Fung, I. Y., Gruber, N., Harrison, D. E., et al. (2002). A large-scale carbon observing plan: *in situ* oceans and atmosphere (LSCOP). *Nat. Tech. Info. Services Springfield*, p. 201.
- Chau, T. T. T., Gehlen, M., and Chevallier, F. (2022). A seamless ensemble-based reconstruction of surface ocean $p\text{CO}_2$ and air-sea CO_2 fluxes over the global coastal and open oceans. *Biogeosciences* 19, 1087–1109. doi: 10.5194/bg-19-1087-2022
- Chau, T. T. T., Gehlen, M., Metzl, N., and Chevallier, F. (2024). CMEMS-LSCE: a global, 0.25°, monthly reconstruction of the surface ocean carbonate system. *Earth System Sci. Data* 16, 121–160. doi: 10.5194/essd-16-121-2024
- Chen, S., Hu, C., Barnes, B. B., Wanninkhof, R., Cai, W. J., Barbero, L., et al. (2019). A machine learning approach to estimate surface ocean $p\text{CO}_2$ from satellite measurements. *Remote Sens. Environ.* 228, 203–226. doi: 10.1016/j.rse.2019.04.019
- Chiodi, A. M., Dunne, J. P., and Harrison, D. E. (2019). Estimating air-sea carbon flux uncertainty over the tropical Pacific: Importance of winds and wind analysis uncertainty. *Global Biogeochemical Cycles* 33, 370–390. doi: 10.1029/2018gb006047
- Curry, R. G., and McCartney, M. S. (2001). Ocean gyre circulation changes associated with the North Atlantic Oscillation. *J. Phys. Oceanography* 31, 3374–3400. doi: 10.1175/1520-0485(2001)031<3374:ogccaw>2.0.co;2
- Cyr, F., Gibb, O., Azetsu-Scott, K., Chassé, J., Galbraith, P., Maillet, G., et al. (2022). Ocean carbonate parameters on the Canadian Atlantic Continental Shelf. *Federated Res. Data Repository*. doi: 10.20383/102.0673
- DeGrandpre, M. D., Körtzinger, A., Send, U., Wallace, D. W., and Bellerby, R. G. J. (2006). Uptake and sequestration of atmospheric CO_2 in the Labrador Sea deep convection region. *Geophysical Res. Lett.* 33, L21S03. doi: 10.1029/2006gl026881
- Denvil-Sommer, A., Gehlen, M., Vrac, M., and Mejia, C. (2019). LSCE-FFNN-v1: A two-step neural network model for the reconstruction of surface ocean $p\text{CO}_2$ over the global ocean. *Geoscientific Model. Dev.* 12, 2091–2105. doi: 10.5194/gmd-12-2091-2019
- DeVries, T. (2014). The oceanic anthropogenic CO_2 sink: Storage, air-sea fluxes, and transports over the industrial era. *Global Biogeochemical Cycles* 28, 631–647. doi: 10.1002/2013gb004739
- DeVries, T. (2022). The ocean carbon cycle. *Annu. Rev. Environ. Resour.* 47, 317–341. doi: 10.1146/annurev-environ-120920-111307
- Dlugokencky, E. J., Mund, J. W., Crotwell, A. M., Crotwell, M. J., and Thoning, K. W. (2021). Atmospheric carbon dioxide dry air mole fractions from the NOAA GML carbon cycle cooperative global air sampling network 1968–2019, version: 2021-02. doi: 10.15138/wkqj-f215
- Dong, Y., Bakker, D. C., and Landschützer, P. (2024). Accuracy of ocean CO_2 uptake estimates at a risk by a reduction in the data collection. *Geophysical Res. Lett.* 51, e2024GL108502. doi: 10.1029/2024gl108502
- Duke, P. J., Hamme, R. C., Ianson, D., Landschützer, P., Ahmed, M. M., Swart, N. C., et al. (2023a). Estimating marine carbon uptake in the northeast Pacific using a neural network approach. *Biogeosciences* 20, 3919–3941. doi: 10.5194/bg-20-3919-2023
- Duke, P. J., Hamme, R. C., Ianson, D., Landschützer, P., Swart, N. C., and Covert, P. A. (2024). High-resolution neural network demonstrates strong CO_2 source-sink juxtaposition in the coastal zone. *J. of Geophysical Research: Oceans* 129, e2024JC021134. doi: 10.1029/2024JC021134
- Duke, P. J., Richaud, B., Arruda, R., Länger, J., Schuler, K., Gooya, P., et al. (2023b). Canada's marine carbon sink: an early career perspective on the state of research and existing knowledge gaps. *Facets* 8, 1–21. doi: 10.1139/facets-2022-0214
- Fang, X., and An, D. (2022). Evaluation on sea surface wind speed product of Fengyun-3D satellite microwave radiation imager using ERA-5 dataset. *Int. J. Remote Sens.* 43, 3671–3691. doi: 10.1080/01431161.2022.2099770
- Fay, A. R., Gregor, L., Landschützer, P., McKinley, G. A., Gruber, N., Gehlen, M., et al. (2021). SeaFlux: harmonization of air-sea CO_2 fluxes from surface $p\text{CO}_2$ data products using a standardized approach. *Earth System Sci. Data* 13, 4693–4710. doi: 10.5194/essd-13-4693-2021
- Fay, A. R., Munro, D. R., McKinley, G. A., Pierrot, D., Sutherland, S. C., Sweeney, C., et al. (2023). Climatological distributions of sea-air $\Delta f\text{CO}_2$ and CO_2 flux densities in the Global Surface Ocean (NCEI Accession 0282251). doi: 10.25921/295g-sn13 (Accessed 01/07/2024).
- Fay, A. R., Munro, D. R., McKinley, G. A., Pierrot, D., Sutherland, S. C., Sweeney, C., et al. (2024). Updated climatological mean $\Delta f\text{CO}_2$ and net sea-air CO_2 flux over the global open ocean regions. *Earth System Sci. Data* 16, 2123–2139. doi: 10.5194/essd-16-2123-2024
- Friedlingstein, P., O'Sullivan, M., Jones, M. W., Andrew, R. M., Gregor, L., Hauck, J., et al. (2022). Global carbon budget 2022. *Earth System Sci. Data* 14, 4811–4900. doi: 10.5194/essd-14-4811-2022
- Friedrich, T., and Oeschler, A. (2009a). Neural network-based estimates of North Atlantic surface $p\text{CO}_2$ from satellite data: A methodological study. *J. Geophysical Research: Oceans* 114, 1–12. doi: 10.1029/2007JC004646
- Friedrich, T., and Oeschler, A. (2009b). Basin-scale $p\text{CO}_2$ maps estimated from ARGO float data: A model study. *J. Geophys. Res.* 114, C10012. doi: 10.1029/2009JC005322
- Fu, Y., Li, F., Karstensen, J., and Wang, C. (2020). A stable Atlantic Meridional Overturning Circulation in a changing North Atlantic Ocean since the 1990s. *Sci. Adv.* 6, eabc7836. doi: 10.1126/sciadv.abc7836
- Gibb, O., Cyr, F., Azetsu-Scott, K., Chassé, J., Galbraith, P. S., Maillet, G., et al. (2023). Spatiotemporal variability of pH and carbonate parameters on the Canadian Atlantic Continental Shelf between 2014 and 2020. *Earth System Sci. Data Discussions* 2023, 1–50. doi: 10.5194/essd-15-4127-2023
- Gloege, L., McKinley, G. A., Landschützer, P., Fay, A. R., Frölicher, T. L., Fyfe, J. C., et al. (2021). Quantifying errors in observationally based estimates of ocean carbon sink variability. *Global Biogeochemical Cycles* 35, e2020GB006788. doi: 10.1029/2020gb006788

- Gregor, L., and Fay, A. (2021). SeaFlux: harmonised sea-air CO₂ fluxes from surface pCO₂ data products using a standardised approach, (2021.04.03). *Zenodo*. doi: 10.5281/zenodo.5482547
- Gregor, L., Lebehoh, A. D., Kok, S., and Scheel Monteiro, P. M. (2019). A comparative assessment of the uncertainties of global surface ocean CO₂ estimates using a machine-learning ensemble (CSIR-ML6 version 2019a)—have we hit the wall? *Geoscientific Model. Dev.* 12, 5113–5136. doi: 10.5194/gmd-12-5113-2019
- Gregor, L., Shutler, J., and Gruber, N. (2024). High-resolution variability of the ocean carbon sink. *Global Biogeochemical Cycles* 38, e2024GB008127. doi: 10.1029/2024gb008127
- Gruber, N., Clement, D., Carter, B. R., Feely, R. A., Van Heuven, S., Hoppema, M., et al. (2019). The oceanic sink for anthropogenic CO₂ from 1994 to 2007. *Science* 363, 1193–1199. doi: 10.1126/science.aau5153
- Guinehut, S., Dhomp, A. L., Larnicol, G., and Le Traon, P. Y. (2012). High resolution 3-D temperature and salinity fields derived from *in situ* and satellite observations. *Ocean Sci.* 8, 845–857. doi: 10.5194/os-8-845-2012
- Hall, M. M., Torres, D. J., and Yashayaev, I. (2013). Absolute velocity along the AR7W section in the Labrador Sea. *Deep Sea Res. Part I: Oceanographic Res. Papers* 72, 72–87. doi: 10.1016/j.dsr.2012.11.005
- Hauck, J., Nissen, C., Landschützer, P., Rödenbeck, C., Bushinsky, S., and Olsen, A. (2023). Sparse observations induce large biases in estimates of the global ocean CO₂ sink: an ocean model subsampling experiment. *Philos. Trans. R. Soc. A* 381, 20220063. doi: 10.1098/rsta.2022.0063
- Hersbach, H., Bell, B., Berrisford, P., Hirahara, S., Horányi, A., Muñoz-Sabater, J., et al. (2020). The ERA5 global reanalysis. *Q. J. R. Meteorological Soc.* 146, 1999–2049. doi: 10.1002/qj.3803
- Iida, Y., Kojima, A., Takatani, Y., Nakano, T., Sugimoto, H., Midorikawa, T., et al. (2015). Trends in pCO₂ and sea–air CO₂ flux over the global open oceans for the last two decades. *J. oceanography* 71, 637–661. doi: 10.1007/s10872-015-0306-4
- Iida, Y., Takatani, Y., Kojima, A., and Ishii, M. (2021). Global trends of ocean CO₂ sink and ocean acidification: an observation-based reconstruction of surface ocean inorganic carbon variables. *J. Oceanography* 77, 323–358. doi: 10.1007/s10872-020-00571-5
- Khatiwala, S., Tanhua, T., Mikaloff Fletcher, S., Gerber, M., Doney, S. C., Graven, H. D., et al. (2013). Global ocean storage of anthropogenic carbon. *Biogeosciences* 10, 2169–2191. doi: 10.5194/bg-10-2169-2013
- Kieke, D., and Yashayaev, I. (2015). Studies of Labrador Sea Water formation and variability in the subpolar North Atlantic in the light of international partnership and collaboration. *Prog. Oceanography* 132, 220–232. doi: 10.1016/j.pocean.2014.12.010
- Koelling, J., Atamanchuk, D., Karstensen, J., Handmann, P., and Wallace, D. W. (2022). Oxygen export to the deep ocean following Labrador Sea Water formation. *Biogeosciences* 19, 437–454. doi: 10.5194/bg-19-437-2022
- Koelling, J., Wallace, D. W., Send, U., and Karstensen, J. (2017). Intense oceanic uptake of oxygen during 2014–2015 winter convection in the Labrador Sea. *Geophysical Res. Lett.* 44, 7855–7864. doi: 10.1002/2017gl073933
- Körtzinger, A., Schimanski, J., Send, U., and Wallace, D. (2004). The ocean takes a deep breath. *Science* 306, 1337–1337. doi: 10.1126/science.1102557
- Körtzinger, A., Send, U., Lampitt, R. S., Hartman, S., Wallace, D. W., Karstensen, J., et al. (2008b). The seasonal pCO₂ cycle at 49°N/16.5°W in the northeastern Atlantic Ocean and what it tells us about biological productivity. *J. Geophysical Research: Oceans* 113, C04020. doi: 10.1029/2007jco04347
- Körtzinger, A., Send, U., Wallace, D. W., Karstensen, J., and DeGrandpre, M. (2008a). Seasonal cycle of O₂ and pCO₂ in the central Labrador Sea: Atmospheric, biological, and physical implications. *Global Biogeochemical Cycles* 22. doi: 10.1029/2007gb003029
- Landschützer, P., Gruber, N., and Bakker, D. C. E. (2016). Decadal variations and trends of the global ocean carbon sink. *Global Biogeochemical Cycles* 30, 1396–1417. doi: 10.1002/2015GB005359
- Landschützer, P., Gruber, N., and Bakker, D. C. E. (2017). An observation-based global monthly gridded sea surface pCO₂ product from 1982 onward and its monthly climatology (NCEI Accession 0160558). Version 4.4 (NOAA National Centers for Environmental Information). doi: 10.7289/V5Z899N6 (Accessed 2019-03-27).
- Landschützer, P., Gruber, N., Bakker, D. C., and Schuster, U. (2014). Recent variability of the global ocean carbon sink. *Global Biogeochemical Cycles* 28, 927–949. doi: 10.1002/2014gb004853
- Landschützer, P., Gruber, N., Bakker, D. C. E., Schuster, U., Nakaoka, S., Payne, M. R., et al. (2013). A neural network-based estimate of the seasonal to inter-annual variability of the Atlantic Ocean carbon sink. *Biogeosciences* 10, 7793–7815. doi: 10.5194/bg-10-7793-2013
- Landschützer, P., Laruelle, G. G., Roobaert, A., and Regnier, P. (2020). A uniform pCO₂ climatology combining open and coastal oceans. *Earth System Sci. Data* 12, 2537–2553. doi: 10.5194/essd-12-2537-2020
- Laruelle, G. G., Landschützer, P., Gruber, N., Ti, J. L., Delille, B., and Regnier, P. (2017). Global high-resolution monthly pCO₂ climatology for the coastal ocean derived from neural network interpolation. *Biogeosciences* 14, 4545–4561. doi: 10.5194/bg-14-4545-2017
- Laruelle, G. G., Lauerwald, R., Pfeil, B., and Regnier, P. (2014). Regionalized global budget of the CO₂ exchange at the air–water interface in continental shelf seas. *Global biogeochemical cycles* 28, 1199–1214. doi: 10.1002/2014gb004832
- Lauderdale, J. M., Dutkiewicz, S., Williams, R. G., and Follows, M. J. (2016). Quantifying the drivers of ocean–atmosphere CO₂ fluxes. *Global Biogeochemical Cycles* 30, 983–999. doi: 10.1002/2016gb005400
- Lüger, H., Wallace, D. W., Körtzinger, A., and Nojiri, Y. (2004). The pCO₂ variability in the midlatitude North Atlantic Ocean during a full annual cycle. *Global Biogeochemical Cycles* 18, GB3023. doi: 10.1029/2003gb002200
- Mackay, N., Watson, A. J., Suntharalingam, P., Chen, Z., and Landschützer, P. (2022). Improved winter data coverage of the Southern Ocean CO₂ sink from extrapolation of summertime observations. *Commun. Earth Environ.* 3, 265. doi: 10.1038/s43247-022-00592-6
- Marshall, J., and Schott, F. (1999). Open-ocean convection: Observations, theory, and models. *Rev. geophysics* 37, 1–64. doi: 10.1029/98rg02739
- Martz, T. R., DeGrandpre, M. D., Strutton, P. G., McGillis, W. R., and Drennan, W. M. (2009). Sea surface pCO₂ and carbon export during the Labrador Sea spring–summer bloom: An *in situ* mass balance approach. *J. Geophysical Research: Oceans* 114, C09008. doi: 10.1029/2008jc005060
- Moore, G. W. K., Pickart, R. S., and Renfrew, I. A. (2008). Buoy observations from the windiest location in the world ocean, Cape Farewell, Greenland. *Geophysical Res. Lett.* 35, L18802. doi: 10.1029/2008gl034845
- Nakaoka, S. I., Aoki, S., Nakazawa, T., Hashida, G., Morimoto, S., Yamanouchi, T., et al. (2006). Temporal and spatial variations of oceanic pCO₂ and air–sea CO₂ flux in the Greenland Sea and the Barents Sea. *Tellus B: Chem. Phys. Meteorology* 58, 148–161. doi: 10.1111/j.1600-0889.2006.00178.x
- Olsen, A., Brown, K. R., Chierici, M., Johannessen, T., and Neill, C. (2008). Sea-surface CO₂ fugacity in the subpolar North Atlantic. *Biogeosciences* 5, 535–547. doi: 10.5194/bg-5-535-2008
- Pérez, F. F., Becker, M., Goris, N., Gehlen, M., López-Mozos, M., Tjiputra, J., et al. (2024). An assessment of CO₂ storage and sea–air fluxes for the Atlantic Ocean and Mediterranean Sea between 1985 and 2018. *Global Biogeochemical Cycles* 38, e2023GB007862. doi: 10.1029/2023GB007862
- Raimondi, L., Matthews, J. B. R., Atamanchuk, D., Azetsu-Scott, K., and Wallace, D. W. (2019). The internal consistency of the marine carbon dioxide system for high latitude shipboard and *in situ* monitoring. *Mar. Chem.* 213, 49–70. doi: 10.1016/j.marchem.2019.03.001
- Raimondi, L., Tanhua, T., Azetsu-Scott, K., Yashayaev, I., and Wallace, D. W. (2021). A 30-year time series of transient tracer-based estimates of anthropogenic carbon in the central Labrador Sea. *J. Geophysical Research: Oceans* 126, e2020JC017092. doi: 10.1029/2020jc017092
- Rödenbeck, C., Bakker, D. C., Gruber, N., Iida, Y., Jacobson, A. R., Jones, S., et al. (2015). Data-based estimates of the ocean carbon sink variability—first results of the Surface Ocean pCO₂ Mapping intercomparison (SOCOM). *Biogeosciences* 12, 7251–7278. doi: 10.5194/bg-12-7251-2015
- Rödenbeck, C., Keeling, R. F., Bakker, D. C., Metzl, N., Olsen, A., Sabine, C., et al. (2013). Global surface–ocean pCO₂ and sea–air CO₂ flux variability from an observation-driven ocean mixed-layer scheme. *Ocean Science* 9, 193–216. doi: 10.5194/os-9-193-2013
- Rodgers, K. B., Schwinger, J., Fassbender, A. J., Landschützer, P., Yamaguchi, R., Frenzel, H., et al. (2023). Seasonal variability of the surface ocean carbon cycle: A synthesis. *Global Biogeochemical Cycles* 37, e2023GB007798. doi: 10.1029/2023GB007798
- Roobaert, A., Laruelle, G. G., Landschützer, P., and Regnier, P. (2018). Uncertainty in the global oceanic CO₂ uptake induced by wind forcing: quantification and spatial analysis. *Biogeosciences* 15, 1701–1720. doi: 10.5194/bg-15-1701-2018
- Roobaert, A., Regnier, P., Landschützer, P., and Laruelle, G. G. (2024). A novel sea surface pCO₂ product for the global coastal ocean resolving trends over 1982–2020. *Earth System Sci. Data* 16, 421–441. doi: 10.5194/essd-16-421-2024
- Rühs, S., Oliver, E. C., Biastoch, A., Böning, C. W., Dowd, M., Getzlaff, K., et al. (2021). Changing spatial patterns of deep convection in the subpolar North Atlantic. *J. Geophysical Research: Oceans* 126, e2021JC017245. doi: 10.1029/2021jc017245
- Sabine, C. L., Feely, R. A., Gruber, N., Key, R. M., Lee, K., Bullister, J. L., et al. (2004). The oceanic sink for anthropogenic CO₂. *science* 305, 367–371. doi: 10.1126/science.1097403
- Schuster, U., McKinley, G. A., Bates, N., Chevallier, F., Doney, S. C., Fay, A. R., et al. (2013). An assessment of the Atlantic and Arctic sea–air CO₂ fluxes 1990–2009. *Biogeosciences* 10, 607–627. doi: 10.5194/bg-10-607-2013
- Steinfeldt, R., Rhein, M., and Kieke, D. (2024). Anthropogenic carbon storage and its decadal changes in the Atlantic between 1990–2020. *Biogeosciences* 21, 3839–3867. doi: 10.5194/bg-21-3839-2024
- Sutton, A. J., Williams, N. L., and Tilbrook, B. (2021). Constraining Southern Ocean CO₂ flux uncertainty using uncrewed surface vehicle observations. *Geophysical Res. Lett.* 48, e2020GL091748. doi: 10.1029/2020gl091748
- Takahashi, T., Sutherland, S. C., Sweeney, C., Poisson, A., Metzl, N., Tilbrook, B., et al. (2002). Global sea–air CO₂ flux based on climatological surface ocean pCO₂, and seasonal biological and temperature effects. *Deep Sea Res. Part II: Topical Stud. Oceanography* 49, 1601–1622. doi: 10.1016/s0967-0645(02)00003-6
- Takahashi, T., Sutherland, S. C., Wanninkhof, R., Sweeney, C., Feely, R., Chipman, D. W., et al. (2009). Climatological mean and decadal change in surface ocean pCO₂, and net sea–air CO₂ flux over the global oceans. *Deep Sea Res. Part II: Topical Stud. Oceanography* 56, 554–577. doi: 10.1016/j.dsr2.2008.12.009

- Telszewski, M., Chazottes, A., Schuster, U., Watson, A. J., Moulin, C., Bakker, D. C. E., et al. (2009). Estimating the monthly $p\text{CO}_2$ distribution in the North Atlantic using a self-organizing neural network. *Biogeosciences* 6, 1405–1421. doi: 10.5194/bg-6-1405-2009
- Terenzi, F., Hall, T. M., Khatiwala, S., Rodehacke, C. B., and LeBel, D. A. (2007). Uptake of natural and anthropogenic carbon by the Labrador Sea. *Geophysical Res. Lett.* 34, L06608. doi: 10.1029/2006gl028543
- Wanninkhof, R. (1992). Relationship between wind speed and gas exchange over the ocean. *J. Geophysical Research: Oceans* 97, 7373–7382. doi: 10.1029/92jc00188
- Wanninkhof, R., Pickers, P. A., Omar, A. M., Sutton, A., Murata, A., Olsen, A., et al. (2019). A surface ocean CO_2 reference network, SOCONET and associated marine boundary layer CO_2 measurements. *Front. Mar. Sci.* 6, 400. doi: 10.3389/fmars.2019.00400
- Watson, A. J., Schuster, U., Shutler, J. D., Holding, T., Ashton, I. G., Landschützer, P., et al. (2020). Revised estimates of ocean-atmosphere CO_2 flux are consistent with ocean carbon inventory. *Nat. Commun.* 11, 4422. doi: 10.1038/s41467-020-18203-3
- Weiss, R. (1974). Carbon dioxide in water and seawater: the solubility of a non-ideal gas. *Mar. Chem.* 2, 203–215. doi: 10.1016/0304-4203(74)90015-2
- Woolf, D. K., Shutler, J. D., Goddijn-Murphy, L., Watson, A. J., Chapron, B., Nightingale, P. D., et al. (2019). Key uncertainties in the recent air-sea flux of CO_2 . *Global Biogeochemical Cycles* 33, 1548–1563. doi: 10.1029/2018GB006041
- Worthy, D. (ECCC), Atmospheric CO_2 at Sable Island by Environment and Climate Change Canada, dataset published as $\text{CO}_2_WSA_surface-insitu_ECCC_data1$ at WDCGG, ver. 2023-08-31-0904 (Reference date*: 2023/06/20).
- Wright, E. E., Bourassa, M. A., Stoffelen, A., and Bidlot, J. R. (2021). Characterizing buoy wind speed error in high winds and varying sea state with ASCAT and ERA5. *Remote Sens.* 13, 4558. doi: 10.3390/rs13224558
- Wrobel-Niedzwiecka, I., Kitowska, M., Makuch, P., and Markuszewski, P. (2022). The Distribution of $p\text{CO}_2$ and Air-Sea CO_2 Fluxes Using FFNN at the Continental Shelf Areas of the Arctic Ocean. *Remote Sens.* 14, 312. doi: 10.3390/rs14020312
- Wu, Y., and Qi, D. (2022). Inconsistency between ship-and Argo float-based $p\text{CO}_2$ at the intense upwelling region of the Drake Passage, Southern Ocean. *Front. Mar. Sci.* 9. doi: 10.3389/fmars.2022.1002398
- Xu, S., Park, K., Wang, Y., Chen, L., Qi, D., and Li, B. (2019). Variations in the summer oceanic $p\text{CO}_2$ and carbon sink in Prydz Bay using the self-organizing map analysis approach. *Biogeosciences* 16, 797–810. doi: 10.5194/bg-16-797-2019
- Yashayev, I., and Loder, J. W. (2017). Further intensification of deep convection in the Labrador Sea in 2016. *Geophysical Res. Lett.* 44, 1429–1438. doi: 10.1002/2016gl071668
- Zantopp, R., Fischer, J., Visbeck, M., and Karstensen, J. (2017). From interannual to decadal: 17 years of boundary current transports at the exit of the Labrador Sea. *J. Geophysical Research: Oceans* 122, 1724–1748. doi: 10.1002/2016jc012271
- Zeng, J., Nojiri, Y., Landschützer, P., Telszewski, M., Nakaoka, S., Landschützer, P., et al. (2014). A global surface ocean $f\text{CO}_2$ climatology based on a feed-forward neural network. *J. Atmospheric Oceanic Technol.* 31, 1838–1849. doi: 10.1175/JTECH-D-13-00137.1